

# Strain effect on adatom binding and diffusion in homo- and heteroepitaxies of Si and Ge on (001) Surfaces

L. Huang,<sup>1</sup> Feng Liu,<sup>2,3</sup> and X. G. Gong<sup>1,4,3</sup><sup>1</sup>*Surface Physics Laboratory and Department of Physics, Fudan University, Shanghai 200433, People's Republic of China*<sup>2</sup>*Department of Materials Science and Engineering, University of Utah, Salt Lake City, Utah 84112, USA*<sup>3</sup>*Interdisciplinary Center for Theoretical Studies, Chinese Academy of Sciences, Beijing 100080, China*<sup>4</sup>*Institute of Solid State Physics, Chinese Academy of Science, Hefei 230031, People's Republic of China*

(Received 2 February 2004; published 22 October 2004)

Strain dependence of adatom binding energies and diffusion barriers in homo- and heteroepitaxies of Si and Ge on (001) surface has been studied using first-principles calculations. In general, Si adatom binding energies and diffusion barriers are larger on Si(001) and Ge(001) surfaces than a Ge adatom, in accordance with decreasing bond strength from Si-Si to Si-Ge and to a Ge-Ge bond. The overall surface diffusion anisotropy of Si and Ge adatoms is found to be comparable on both Si(001) and Ge(001). The essentially linear dependence of binding energies and diffusion barriers on external strain is reproduced in all the cases, giving strong evidence for *a priori* quantitative prediction of the effect of external strain on adatom binding and surface diffusion.

DOI: 10.1103/PhysRevB.70.155320

PACS number(s): 68.35.Fx, 81.05.Tp, 82.20.Kh

## I. INTRODUCTION

The epitaxial growth of elemental semiconductors (Si and Ge) is of considerable scientific and technological significance, because Si and Ge are base materials used in electronic devices and serve also as ideal model systems for studying semiconductor surfaces and growth. Misfit strain is inherently present in heteroepitaxial growth of SiGe thin films due to the 4.2% lattice mismatch between the two materials. Consequently, the effect of strain on growth of SiGe films has been extensively studied, both experimentally and theoretically.<sup>1,2</sup> So far, a majority of studies have been devoted to the strain effect on surface and growth thermodynamics, in particular for the growth of SiGe film on a Si(001) substrate,<sup>1,2</sup> while less attention has been paid to the strain effect on growth kinetics, with limited theoretical studies on the effect of strain on surface diffusion for Si and Ge systems.<sup>3-5</sup>

Previously, we have carried out first-principles calculations to investigate the effect of strain on surface self-diffusion on Si(001). We showed that the effect of strain on surface diffusion is *inherently* correlated with the intrinsic surface stress induced by the adatom along its diffusion pathways. The diffusion barrier depends linearly on the external strain. Furthermore, we proposed a simple generic method to predict quantitatively the change of surface diffusion under a given external strain by first-principles calculations of adatom-induced surface stress on an unstrained surface. Recently, Walle *et al.* have carried out first-principles calculations to study the effect of strain on diffusion of a Ge adatom on Si(001) and Ge(001) surfaces.<sup>4</sup> The dependence of the diffusion barrier on external strain from their calculations for a Ge adatom on Si(001) and Ge(001) is noticeably less linear than what we found for a Si adatom on Si(001).<sup>3</sup>

To further confirm the physical (linear) dependence of the surface diffusion barrier on external strain that we discovered earlier for Si self-diffusion on Si(001) (Ref. 3) and to provide

a complete set of first-principles values of adatom binding energies and diffusion barriers, as well as their strain dependence for homo- and heteroepitaxial growth on Si(001) and Ge(001) surfaces, we present here comprehensive first-principles calculations of the strain dependence of adatom binding energies and diffusion barriers for Ge on Si(001), Si on Ge(001), and Ge on Ge(001) surfaces. In general, our calculations show that the surface binding energies of a Si adatom is higher than those of a Ge adatom, and both adatoms bind more strongly to Si(001) than to Ge(001). The diffusion barriers of Si and Ge adatoms on Si(001) are significantly higher than those on Ge(001), and the diffusion barriers for a Si adatom are higher than those for a Ge adatom on the same type of surface. These results are in good agreement with the common intuition of decreasing bond strength from Si-Si to Si-Ge and to a Ge-Ge bond, and they agree with available experimental data.<sup>6-9</sup> The surface diffusion anisotropy in all the systems studied is comparable. Furthermore, the linear dependence of the diffusion barriers on the external strain is reproduced in all the cases. To determine the range of validity of such linearity, calculations are extended to larger strain to see where the linearity breaks down. Surprisingly, the linear dependence is found to sustain up to rather large strain in some cases. Strain is found to have a much smaller influence on the saddle-point energy than on the minimum-point (binding) energy.

## II. COMPUTATIONAL DETAILS

All the calculations are carried out using the ultrasoft pseudopotential total-energy method within the local-density approximation (LDA), following the procedure used in our previous studies.<sup>3</sup> To ensure a consistent set of convergence criteria for systems containing both Si and Ge, the Kohn-Sham orbitals are expanded in plane waves with an energy cutoff of 11 Ry. We use a supercell consisting of a ten-

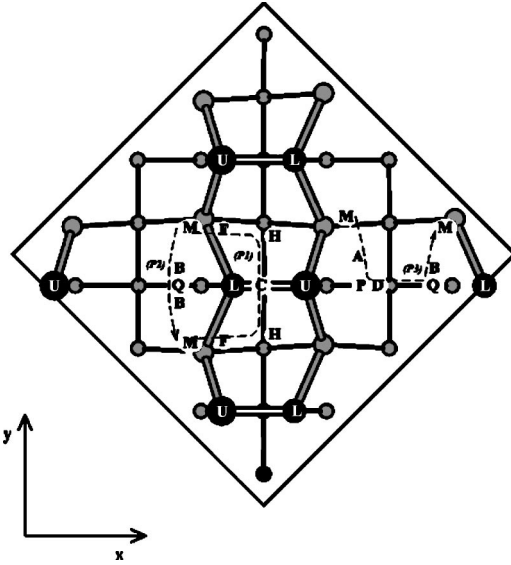


FIG. 1. Top view of the Si(001) or Ge(001)- $p(2 \times 2)$  surface unit cell. The solid circles are the first-layer atoms, the larger shaded circles are the second-layer atoms, and the smaller shaded circles are the third-layer atoms. *U* and *L* denote the upper and lower atoms, respectively, in the buckled surface dimers. The labels indicate the approximate positions of minimum sites (*M*, *H*, *Q*, and *P*) and saddle points (*F*, *C*, *A*, *D*, and *B*). The arrowed dashed lines indicate different pathways: *P1*(*MFHCHFM*), along the top of the dimer rows; *P2*(*MBQBM*), along the edge of the trough between the dimer rows; and *P3*(*MAPDQBM*), perpendicular to the dimer rows.

atomic-layer slab with a  $p(\sqrt{8} \times \sqrt{8})R45^\circ$  unit cell in lateral directions (eight atoms per layer) and a seven-atomic-layer vacuum to model the Si(001) and Ge(001) surfaces. The atoms in the surface layer form a  $p(2 \times 2)$  reconstruction, as shown in Fig. 1. A Si (Ge) adatom is placed on both the top and bottom surfaces of the slab to retain the inversion symmetry of the supercell. Coordinates of all the atoms are optimized during the structural relaxation, except the two innermost layers that are kept fixed. The potential-energy surface (PES) of the adatom on the unstrained and strained surfaces is mapped out by conjugate gradient minimization, up to a precision of  $10^{-4}$  eV in total-energy difference and with forces on the remaining atoms converged to 0.01 eV/Å. The unstrained Si(001) and Ge(001) surfaces correspond to the calculated bulk lattice constant of 5.39 Å and 5.63 Å, respectively. Two special *K* points are used for the Brillouin-zone sampling. Tests have been done to make sure that all the results are converged with respect to energy cutoff, system size, and *k*-points sampling.

A common practice, when addressing adatom diffusion, is to map out the PES via placing an adatom laterally over a set of equidistant grid points. At each point, the *z* coordinate of the adatom is optimized along with the full coordinates of all other atoms. To accurately locate all the minima and saddle points in the complex PES and hence accurately determine the diffusion barriers for different diffusion pathways, the exact location and energy of a (local) minimum site are subsequently determined by fully relaxing all the degrees of

TABLE I. Adsorption energies in eV for Si and Ge adatoms at (local) minimum sites on Si(001) and Ge(001) surfaces, relative to the absolute minimum *M* site.

Site	Si/Si(001) <sup>a</sup>	Ge/Si(001)	Si/Ge(001)	Ge/Ge(001)
<i>M</i>	0	0	0	0
<i>H</i>	0.25	0.19	0.15	0.14
<i>Q</i>	0.50	0.64	0.28	0.25
<i>P</i>	0.74	0.88	0.55	0.51

<sup>a</sup>Values are taken from Ref. 3.

freedom of all the atoms (including the adatom), starting from the nearby minimum grid point (i.e., the grid point at which the adatom binding energy is the lowest locally). The saddle point (the transition state) between any two minima and hence the diffusion barrier are then identified using the nudged elastic band (NEB) method.<sup>10</sup>

### III. RESULTS AND DISCUSSION

#### A. Adatom binding and diffusion on unstrained surfaces

As expected, the resulting PES's for Si/Ge(001), Ge/Si(001), and Ge/Ge(001) systems exhibit qualitatively similar features to that of a Si adatom on Si(001). There exist four minimum sites (*M*, *H*, *Q*, and *P*) and five saddle points (*F*, *C*, *B*, *A*, and *D*), as indicated in Fig. 1. The absolute minimum is located at the *M* site. The binding energies are -5.24 eV for Si/Si(001), -4.81 eV for Ge/Si(001), -4.94 eV for Si/Ge(001), and -4.47 eV for Ge/Ge(001), respectively. The relative energies of other local minima, *H*, *Q*, and *P*, with respect to *M*, are listed in Table I. It must be noted that the LDA methods are known to overestimate the binding energies and the results have a systematic error. The general trend, however, is more reliable. We found that the binding energies of a Si adatom is higher than those of a Ge adatom on the same surface, and both adatoms bind more strongly to Si(001) than to Ge(001). The binding energy of a Si adatom on Ge(001) is about the same as that of a Ge adatom on Si(001). These findings follow the common intuition of decreasing bond strength from Si-Si to Si-Ge and to a Ge-Ge bond. In fact, our calculated ratio of adatom binding energies of Si/Si(001) to Ge/Ge(001) and of Ge/Si(001) [or Si/Ge(001)] to Ge/Ge(001) is 1.17 and 1.08 (or 1.11), respectively, which are in good quantitative agreement with the ratio of experimental cohesive energies of Si to Ge and of SiGe (average of the two) to Ge, which is 1.20 and 1.10, respectively.<sup>11</sup> The same trend was also obtained by Mae<sup>12</sup> using the embedded-atom potential.

The complex PES's lead to multiple diffusion pathways. For each combination of the system, we particularly find two possible low-barrier paths for diffusions parallel to the dimer rows, *P1*(*MFHCHFM*) and *P2*(*MBQBM*), and one possible path perpendicular to the dimer rows, *P3*(*MAPDQBM*). Although the binding sites, adsorption geometries, and diffusion pathways of Si and Ge adatoms on the reconstructed Si(001) and Ge(001) surfaces resemble each other, the ener-

TABLE II. Diffusion barriers ( $E_b^0$ ) and  $A\Delta\sigma_{xx}$  ( $A\Delta\sigma_{yy}$ ) for Si and Ge adatom diffusion on unstrained Si(001) and Ge(001). Values in the parentheses are the slopes obtained by linear fits to the calculated points (Figs. 3–5), which are in accordance with the numbers predicted by the unstrained surface calculations. All energies are in eV.

		Si/Si(001) <sup>a</sup>	Ge/Si(001)	Si/Ge(001)	Ge/Ge(001)
$E_b^0$	$P1$	0.65	0.617	0.591	0.526
	$P2$	0.66	0.709	0.435	0.370
	$P3$	1.19	1.175	1.054	0.899
$A\Delta\sigma_{xx}$	$P1$	0.94	0.76 (0.81)	−0.95 (−0.91)	−0.48 (−0.44)
	$P2$	2.43	2.03 (2.33)	2.51 ( 2.29)	1.35 ( 1.42)
	$P3$	3.32	2.39 (2.43)	−0.20 (−0.16)	1.81 ( 1.89)
$A\Delta\sigma_{yy}$	$P1$	−6.23	−5.30 (−5.45)	−7.14 (−6.80)	−5.67 (−5.55)
	$P2$	−0.15	−0.30 (−0.20)	−0.64 (−0.72)	−0.87 (−0.78)
	$P3$	−6.60	−6.37 (−6.34)	−8.64 (−8.73)	−5.58 (−5.41)

<sup>a</sup>Values are taken from Ref. 3.

getics and diffusion dynamics are quantitatively different due to the chemical difference of Si and Ge. In Table II, we present the calculated diffusion barriers for a Ge adatom on unstrained Si(001) and a Si (Ge) adatom on unstrained Ge(001). For comparison, previously reported values for Si/Si(001) (Ref. 3) are included.

From our calculations, we make the following observations. (1) In all three systems, i.e., Ge/Si(001), Si/Ge(001), and Ge/Ge(001), the adatom diffusion is anisotropic, with the fast diffusion direction being along the dimer row, the same as in the case of Si adatom diffusion on Si(001).<sup>3,6,13</sup> The differences of barriers between path  $P1$  ( $P2$ ) and  $P3$  in each of the systems are all at 0.55 eV or so, and the overall anisotropy is thus comparable with each other (about three orders of magnitude at room temperature). These are in good agreement with previous calculations<sup>3,13,14</sup> and experiments.<sup>6–9</sup> (2) The microscopic details of the adatom motion along the dimer row on Ge(001), however, turn out to be somewhat different from that on Si(001). The Si (Ge) adatom seems to have a good chance to diffuse along the trough edge between the dimer rows ( $P2$ ) on Ge(001), in contrast with the behavior on Si(001), where diffusion is predominantly over the top of the dimer row ( $P1$ ).<sup>3,13</sup> For Si/Si(001) and Ge/Si(001), the barriers of  $P1$  and  $P2$  are nearly degenerate, with  $P1$  slightly lower than  $P2$ , whereas for Si/Ge(001) and Ge/Ge(001), the barriers of  $P1$  and  $P2$  differ substantially, with  $P2$  much lower than  $P1$ . (3) The diffusion barriers on Ge(001) are significantly lower than on Si(001), and Ge adatom diffusion has slightly lower barriers than Si adatom diffusion on the same surfaces, again reflecting the lower cohesive energy of Ge as compared to Si. Our calculated diffusion barriers of 0.65 eV (Ref. 3) for Si on Si(001) and 0.37 eV for Ge on Ge(001) agree well with available experiments, which are, respectively, 0.67 eV for Si on Si(001) (Ref. 6) and  $0.47 \pm 0.12$  eV for Ge on Ge(001),<sup>9</sup> and with previous calculations.<sup>13</sup> Furthermore, we note that the same qualitative trend has also been observed experimentally for addimer diffusion.<sup>15,16</sup> (4) For Ge adatom diffusion on Si(001), the diffusion barrier along the top of the dimer rows is estimated to be 0.617 eV, in excellent

agreement with the theoretical<sup>14</sup> and experimental<sup>7,8</sup> result of 0.62 eV, while Walle *et al.* have obtained a lower diffusion barrier of 0.45 eV (Fig. 3 in Ref. 4). It is worth mentioning that different starting configurations of  $c(4 \times 2)$  and  $p(2 \times 2)$  reconstruction have been used in Ref. 4 and the present work, respectively. As has been discussed earlier,<sup>17,18</sup> the diffusion barriers might be sensitive to the local tilting of dimers. (5) Finally, we observe that when a Si (Ge) adatom diffuses into the dimer bridge site ( $C$  site in Fig. 1), it spontaneously opens the otherwise closed dimers on Ge(001), which is necessary for a new layer to form.<sup>19</sup> But in contrast, the presence of an adatom directly above the surface dimer on Si(001) does not lead to the dimer opening.<sup>3,13</sup>

## B. Adatom binding and diffusion on strained surfaces

To investigate how strain affects adatom binding and surface diffusion, the changes of binding energy and diffusion barrier are examined under different strain conditions for Si and Ge surfaces. We have applied compressive and tensile strain up to 2%, uniaxially or biaxially,  $\epsilon_{bi}$ , to the adatom-adsorbed  $p(2 \times 2)$  Si(001) and Ge(001) surfaces. The uniaxial strain is applied in the direction either along the surface dimer bond,  $\epsilon_{xx}$ , or perpendicular,  $\epsilon_{yy}$ . On every strained surface, diffusion barriers are again determined by energy minimization and by the NEB method.<sup>10</sup>

Figure 2 shows the calculated binding energies for an adatom at the global minimum site  $M$  as a function of external strain. The tensile stress is positive. It is interesting to note that there is a linear dependence between the binding energy and external strain, the same as the behavior of molecular adsorption energy on a strained metal surface.<sup>20</sup> The linear dependence can be understood within the scheme of linear elastic theory. The binding energy with external strain  $\epsilon^{\text{ext}}$  can be written as  $E_{\text{ad}} = E_{\text{ad}}^0 + A\sigma\epsilon^{\text{ext}}$ , where  $E_{\text{ad}}^0$  is the binding energy on an unstrained surface,  $A$  is the surface area, and  $\sigma$  is the surface stress tensor induced by the adatom.<sup>20</sup> Qualitatively, adatom binding energy depends linearly on external strain; quantitatively, it depends on the magnitude of the surface stress that the adatom induces at the adsorption site. It is

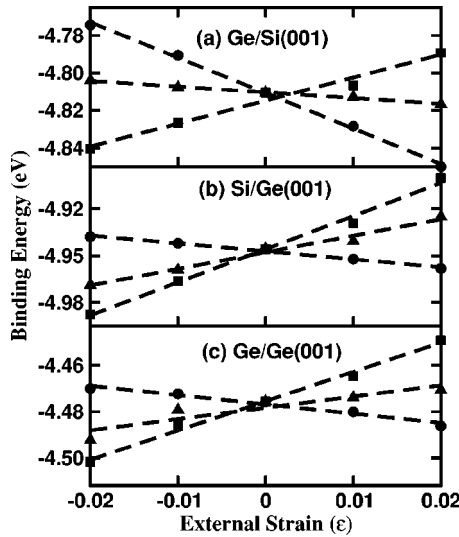


FIG. 2. Strain dependence of the binding energies for a Ge adatom on Si(001) and a Si (Ge) adatom on Ge(001) at the absolute minimum site  $M$ . Circles: uniaxial strain along the dimer rows,  $\epsilon_{xx}$ ; squares: uniaxial strain perpendicular to dimer rows,  $\epsilon_{yy}$ ; triangle: biaxial strain,  $\epsilon_{bi}$ . Dashed lines represent the best linear fits.

rather substantial in all the systems we studied, here up to  $\sim 0.05$  eV for a  $\pm 2\%$  strain. A compressive (or tensile) strain may either increase or decrease the adatom binding to the substrate, as reflected by the opposite effects of  $\epsilon_{xx}$  versus  $\epsilon_{yy}$  in Fig. 2. If an adatom induces a tensile surface stress, the binding energy increases with increasing external strain; the reverse is true if it induces a compressive surface stress.

The dependence of the diffusion barriers along the path  $P1$ ,  $P2$ , and  $P3$  on external strain of  $\epsilon_{xx}$ ,  $\epsilon_{yy}$ , and  $\epsilon_{bi}$  is plotted, respectively, in Fig. 3 for the Ge/Si(001) system. Figures 4 and 5 show the same results for Si/Ge(001) and Ge/Ge(001) systems, respectively. The features exhibited in

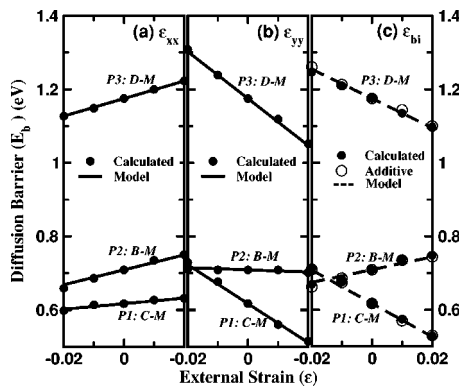


FIG. 3. The diffusion barriers of different pathways ( $P1$ ,  $P2$ , and  $P3$ ) for Ge on Si(001) as a function of the externally applied strain. (a) Uniaxial strain along the dimer rows,  $\epsilon_{xx}$ ; (b) uniaxial strain perpendicular to dimer rows,  $\epsilon_{yy}$ ; and (c) biaxial strain,  $\epsilon_{bi}$ . Solid circles are the calculated diffusion barriers on strained surfaces. The straight lines are predictions, using  $E_b = E_b^0 + \Delta\sigma\epsilon^{\text{ext}}$ , where  $E_b^0$  and  $\Delta\sigma$  are calculated from the unstrained surfaces with the adatom at the minimum and saddle points. The open circles and dashed lines in (c) are obtained by adding the results of (a) and (b).

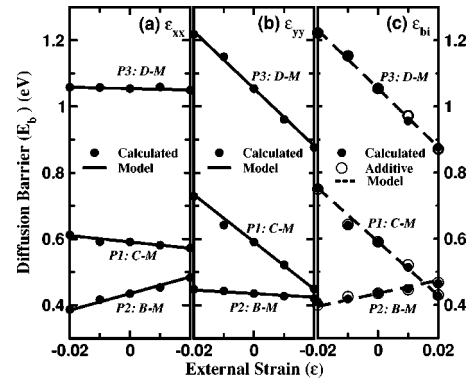


FIG. 4. Same as Fig. 3 for the diffusion barriers of a Si adatom on a Ge(001) surface.

Figs. 3–5 have several significant implications. First, the diffusion barriers show the same trend as binding energies scaling linearly with the external strain in all the cases. They support that an *a priori* quantitative prediction of the effect of external strain on surface diffusion can be achieved by the linear approximation as proposed before for the Si/Si(001) system.<sup>3</sup> The diffusion barrier is thus given by  $E_b = E_b^0 + \Delta\sigma\epsilon^{\text{ext}}$ ,<sup>21</sup> where  $\Delta\sigma$  is the difference of the intrinsic surface stress induced by the adatom at the saddle and minimum point. As shown in Figs. 3–5, the theoretical predictions using the values of  $E_b^0$  and  $\Delta\sigma$  obtained from the unstrained surface calculations (solid straight lines) are all in excellent agreement with the results obtained from a large amount of strained surface calculations (data points of solid circles). Second, the effect of strain on diffusion is quantitatively rather significant in all these systems. A 2% strain (compressive or tensile) can change the diffusion barrier as large as 170 meV [see, e.g., the change of the barrier for path  $P3$  by  $\epsilon_{yy}$  in Fig. 4(b)], which translates to an increase or decrease of diffusion rate by more than a few times at the typical growth temperature of 500°C. Third, the effect of a given external strain is highly pathway- and system-dependent. The strength and sign of the dependence are determined by  $\Delta\sigma$ , which are listed in Table II. Fourth, the effect of strain is additive. Figures 3(c), 4(c), and 5(c), show clearly that the diffusion barriers under biaxial strain (solid circles) agree very well with the additions of the effects of uniaxial strains

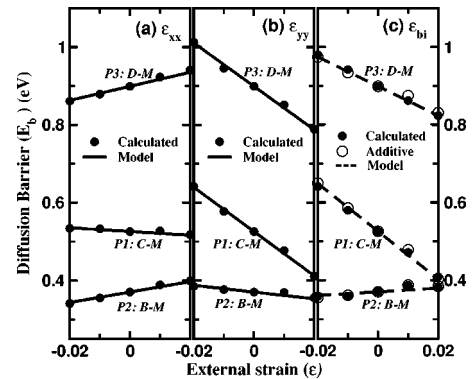


FIG. 5. Same as Fig. 3 for the diffusion barriers of a Ge adatom on a Ge(001) surface.



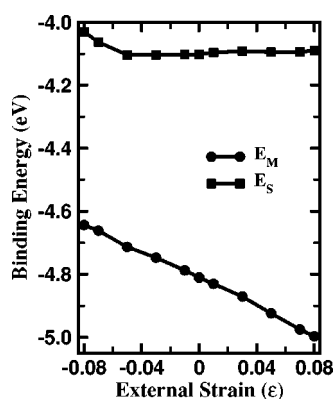


FIG. 6. Strain dependence of the binding energies of a Ge adatom at the minimum site  $E_M$  and saddle point ( $B$ )  $E_S$  on Si(001), respectively, with the external strain exerted perpendicular to the dimer rows. Lines have been drawn to connect data points for clarity.

(open circles). The additive property of the strain effects allows us to achieve the full control of surface diffusion by applying and manipulating only the uniaxial strain, which might be easier to engineer experimentally. Finally, the surface-diffusion anisotropy on both Si(001) and Ge(001) can be enhanced because of the strain-induced change of diffusion pathways.

One can expect that the linear approximation is applicable as long as the multiaatomic distortions involved in the diffusion processes remain within the linear regime. It is important to determine the range of linearity, because it must fail beyond a critical large strain limit. Higher-order terms in  $\epsilon$  must then be included to adequately describe the diffusion barrier. We have done some calculations to extend the strain to a much larger amount to determine where the linearity breaks down. Consider the fact that the linear dependence of the diffusion barrier on strain results from the strain dependence of adatom adsorption energies at both the minimum and the saddle points. We show in Fig. 6 the variation of the adsorption energy of a Ge adatom on Si(001) at the minimum site  $E_M$  together with that at the saddle point ( $B$ )  $E_S$  as a function of the external strain applied perpendicular to the dimer row. Interestingly, the two behave quite differently. Particularly in this case, the linearity breaks down theoretically much sooner at the saddle point (at  $\sim 5\%$  strain) than at the minimum site (sustaining up to as large as  $\sim 8\%$  strain). This indicates that a significant change in the multiaatomic configurations involved in the adatom adsorption at the saddle point occurs at  $\sim 5\%$  strain. Quantitatively, the strain

has a much smaller influence on the saddle-point energy ( $E_S$ ) than on the minimum-point energy ( $E_M$ ), in agreement with earlier predictions for metal surfaces.<sup>22,23</sup> In general, one can expect that the range of linearity can be valid up to a few percent of strain. It depends on the system, the diffusion pathway, and the type of strain (uniaxial versus biaxial) applied. We note that the maximum misfit strain in heteroepitaxial growth of Si and Ge systems is 4%, within the theoretical limit of the linear regime, but in the case of Ge island growth on Si, the compressive strain around the Ge islands may exceed 4%.

#### IV. SUMMARY

In summary we have carried out a comprehensive systematic first-principles study of the strain dependence of adatom binding and diffusion for Ge/Si(001), Si/Ge(001), and Ge/Ge(001) systems. In general, our calculations show that the binding energies of a Si adatom are higher than those of a Ge adatom and both adatoms bind more strongly to Si(001) than to Ge(001). The diffusion barriers of Si and Ge adatoms on Si(001) are significantly higher than those on Ge(001), and diffusion barriers for a Si adatom are higher than those for a Ge adatom on the same type of surface. These results are in good agreement with the common intuition of decreasing bond strength from Si-Si to Si-Ge and to a Ge-Ge bond. The surface diffusion anisotropy in all the systems studied is comparable. Furthermore, the linear dependence of the binding energies and diffusion barriers on the external strain is reproduced in all the cases, giving strong evidence for *a priori* quantitative prediction of the effect of external strain on surface binding and diffusion. The linear dependence is found to sustain theoretically up to rather large strain in some cases. Strain is found to have a much smaller influence on the saddle-point energy than on the minimum-point (binding) energy. These results, together with our earlier study on the Si/Si(001) system,<sup>3</sup> provide a complete set of first-principles values of adatom binding energies and diffusion barriers as well as their strain dependence for homo- and heteroepitaxial growth on Si(001) and Ge(001) surfaces.

#### ACKNOWLEDGMENTS

L.H. thanks X. Ge and M. Ji for helpful discussions and X. Wang for a critical reading of the manuscript. The work is supported by the National Natural Science Foundation of China, the special funds for major state basic research project, and CAS projects. The work of F.L. is supported by the DOE and the NSF.

<sup>1</sup>For a review on early-stage growth of Ge on Si(001), see, e.g., Feng Liu, Fang Wu, and M. G. Lagally Chem. Rev. (Washington, D.C.) **97**, 1045 (1997).

<sup>2</sup>For a review on late-stage growth of SiGe on Si(001), see, e.g., Feng Liu and M. G. Lagally, Surf. Sci. **386**, 169 (1997).

<sup>3</sup>D. J. Shu, Feng Liu, and X. G. Gong, Phys. Rev. B **64**, 245410

(2001).

<sup>4</sup>A. van de Walle, M. Asta, and P. W. Voorhees, Phys. Rev. B **67**, 041308 (2003).

<sup>5</sup>K. Schroeder, A. Antons, R. Berger, and S. Blügel, Phys. Rev. Lett. **88**, 046101 (2002).

<sup>6</sup>Y.-W. Mo, J. Kleiner, M. B. Webb, and M. G. Lagally, Phys. Rev.

- Lett. **66**, 1998 (1991).
- <sup>7</sup>Y.-W. Mo and M. G. Lagally, Surf. Sci. **248**, 313 (1991).
- <sup>8</sup>M. G. Lagally, Jpn. J. Appl. Phys., Part 1 Part 1 **32**, 1493 (1993).
- <sup>9</sup>H. J. W. Zandvliet (unpublished).
- <sup>10</sup>H. Jonsson, G. Mills, and K. W. Hacıobsen, in *Classical and Quantum Dynamics in Condensed Phase Simulation*, edited by B. J. Berne, G. Ciccotti, and D. F. Coker (World Scientific, Singapore, 1998), Chap. 16.
- <sup>11</sup>C. Kittel, *Introduction to Solid State Physics* (Wiley, New York, 1996), p. 57.
- <sup>12</sup>K. Mae, Thin Solid Films **395**, 235 (2001).
- <sup>13</sup>G. Brocks, P. J. Kelly, and R. Car, Phys. Rev. Lett. **66**, 1729 (1991).
- <sup>14</sup>V. Milman, D. E. Jesson, S. J. Pennycook, M. C. Payne, M. H. Lee, and I. Stich, Phys. Rev. B **50**, 2663 (1994).
- <sup>15</sup>W. Wulfskel, B. J. Hatink, H. J. W. Zandvliet, G. Rosenfeld, and B. Poelsema, Phys. Rev. Lett. **79**, 2494 (1997).
- <sup>16</sup>T. V. Afanasieva, S. Yu. Bulavenko, I. F. Koval, and H. J. W. Zandvliet, J. Appl. Phys. **93**, 1452 (2003).
- <sup>17</sup>Q.-M. Zhang, C. Roland, P. Boguslawski, and J. Bernhole, Phys. Rev. Lett. **75**, 101 (1995).
- <sup>18</sup>G. M. Dalpian, A. Fazzio, and Antônio J. R. da Silva, Phys. Rev. B **63**, 205303 (2001).
- <sup>19</sup>D. Srivastava, B. J. Garrison, and D. W. Brenner, Phys. Rev. Lett. **63**, 302 (1989).
- <sup>20</sup>R. Pala and Feng Liu, J. Chem. Phys. (to be published).
- <sup>21</sup>H. T. Dobbs, A. Zangwill, and D. D. Vvedensky, in *Surface Diffusion: Atomistic and Collective Process*, edited by M. Tringides (Plenum, New York, 1997), p. 263.
- <sup>22</sup>R. F. Sabiryanov, M. I. Larsson, K. J. Cho, W. D. Nix, and B. M. Clemens, Phys. Rev. B **67**, 125412 (2003).
- <sup>23</sup>Wei Xiao, P. Alex Greaney, and D. C. Chrzan, Phys. Rev. Lett. **90**, 156102 (2003).